Plasmonic Adder/Subtractor Module Based on a Ring Resonator Filter

M. Janipour*, M. A. Karami*(C.A.) and A. Zia*

Abstract: A four port network adder-subtractor module, for surface plasmon polariton (SPP) waves based on a ring resonator filter is proposed. The functionality of module is achieved by the phase difference manipulation of guided SPPs through different arms connected to the ring resonator. The module is designed using the concepts of a basic two-port device proposed in this paper. It is shown that two port network eliminates odd, and transmits even SPP modes of a single source. Moreover, in the case of four-port adder (with two individual sources), it is elucidated that according to the location of each output port, one can achieve the consequent added or subtracted outputs, correspondingly. Two distinct peaks are observed in the transmission spectrum of adder and subtractor outputs, where increasing the individual source phase difference, leads to a red shift in the adder output, and a blue shift in the subtractor output peaks. The proposed module can be used as the building block for implementing arithmetic operations in plasmonic integrated circuits. The transmission line theory verifies the numerical simulation results, and demonstrates the functionality of the adder/subtractor module.

Keywords: Plasmonics, Ring resonator, Transmission line model.

1 Introduction

Subwavelength nature of plasmonic waveguides makes them a proper candidate for miniaturized integrated photonic circuits [1, 2]. In order to transport SPP waves, various metallic nanostructures such as Insulator-Metal-Insulator (IMI) waveguides [3], nanoparticles [2-4], domino structures [5], grooves, and wedges [6-8], and Metal-Insulator-Metal (MIM) waveguides [3, 9] have been investigated. In addition to the simplicity of fabrication, the high degree of confining optical energy in a compact size has made MIM geometry the most attractive one among the other solutions [10]. Moreover, fundamental plasmonic elements such as filters [11-13], demultiplixers [14, 15], nanoantennas [16] are implemented using the similar topologies. In contrast with IMI waveguides which support long distance non-confined modes [17, 18], MIM structures show large losses in SPP propagation with the propagation length of about ten microns [6, 19]. Building all-optical logic elements is of the interest of engineers to realize faster arithmetic operations [20, 21]. Since the optical devices are free from RC delay as the intrinsic drawback of electronic devices, several studies have been conducted to make optical logic devices. Moreover, increasing the static and dynamic power consumption in electronic integrated circuits drives the industry to replace electronic logic devices with the photonics ones. Making a high performance logic adder can lead to the implementation of other complex logic elements.

Recently, MIM waveguides have been used for implementing the miniaturized plasmonic logic gates [21, 22, 23]. The presented study proposes a ring resonator based adder-subtractor, as the building block for MIM plasmonic circuits. The theory of transmission line method (TLM) [24], and numerical finite difference time domain (FDTD) calculations are used to verify the functionality of the presented structure.

2 Theoretical Model

Using microwave concepts for Rat-race couplers/hybrids, the phase variation of waves passing through a ring resonator, can be employed to make an adder-subtractor module in plasmonic integrated circuits [25]. Since the phase of a SPP wave is proportional to the physical length of the MIM waveguide medium, the phase variation of SPPs can be controlled via the waveguide physical length [25]. Hence, phase dependency of SPPs in MIM structures may be used for the realization of adding operation for two distinct SPP sources. For instance, in a MIM waveguide based T-junction combiner with two unequal waveguide arms, if

Iranian Journal of Electrical & Electronic Engineering, 2016.
Paper received 29 September 2015 and accepted 14 February 2016.
* The Authors are with the School of Electrical Engineering, Iran University of Science and Technology, Narmak, Tehran, Iran.
E-mail: karami@iust.ac.ir

the phase difference between waveguide arms is 0 or π radians, the input SPPs at the junction can be added or subtracted, respectively. In order to show the impact of phase difference in the adding operation, a basic two-port ring resonator based metallic structure is considered to be composed of a power combiner and a power divider T-junction. Fig. 1(a), and Fig. 1(b) show the schematic representation of a basic ring resonator based two-port metallic nanostructure, and its equivalent circuit using TLM theory, with ($l_3 = l_3' + l_3''$) and ($l_2 = l_2' + l_2''$), respectively. The R_{ave}=210 nm (average radius) and the thickness of the air gap is constant value of w = 50 nm, which causes a unique characteristic impedance (Z_0) for the whole structure. The applied optical energy at port-1 is divided into two equal parts according to the equal characteristic impedances of the branches. The resonant wavelength of the ring resonator, λ_r= 1860 nm, can be found in [11, 26]. One portion of the input SPP wave passes through $l_3' = \lambda_r / 8$ arm of the divider part and $l_3'' = \lambda_r / 8$ of the combiner part. The other portion of the SPP wave passes through $l_2' = 3\lambda_r / 8$ arm of the divider part and $l_2'' = 3\lambda_r / 8$ arm of the combiner part.

Hence, the total physical lengths associated to l_3, and l_2 are equal to $\lambda_r/4$, and $3\lambda_r/4$, respectively. Here, $\beta_{SPP}=Re[\beta_{SPP}]+iIm[\beta_{SPP}]$ is the SPP propagation constant in the MIM waveguide, so that $Re[\beta_{SPP}]=2\pi/\lambda_{SPP}$ and $Im[\beta_{SPP}]=1/2\ L_{SPP}$, where λ_{SPP} and L_{SPP} correspond to SPP wavelength and propagation length, respectively. The electrical phase proportional to l_2 and l_3 can be written as [1]:

$$\theta_n = -\beta_{SPP} l_n = -\left(\frac{2\pi}{\lambda_{SPP}} + i\frac{1}{L_{SPP}}\right) l_n,\ n=2,3 \qquad (1)$$

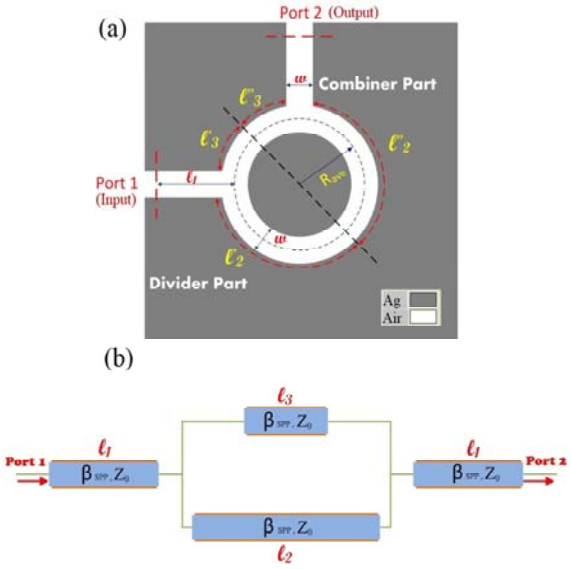

Fig. 1 (a) Schematic representation of the basic two port MIM structure, (b) Transmission line equivalent model for the proposed structure.

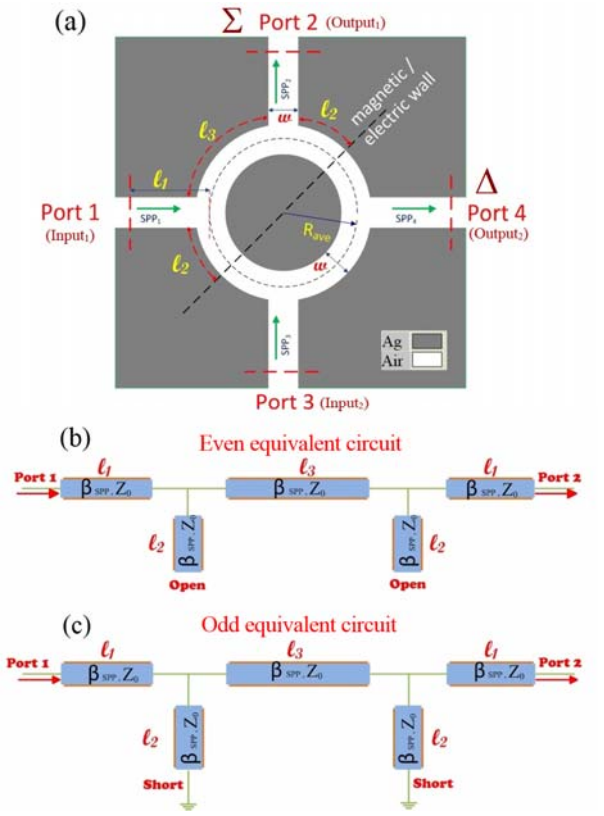

Fig. 2 (a) Schematic representation of the four port MIM adder-subtractor module. (b) Even, and (c) odd transmission line equivalent of the four port element.

Thus, the SPPs transmitted through the MIM arms have the phase difference of $\Delta\theta=\theta_2-\theta_3$. Due to the phase difference, the transmitted SPP at the combiner junction port (i.e., the output port) can be equal to the summation or subtraction of the branched SPP waves, based on the $\Delta\theta$ value. This means that, if the phase difference is $\Delta\theta=2\pi k$, with k = 0, 1, 2, etc., the addition operation, and if $\Delta\theta=(2k+1)\pi$, the subtraction operation can be achieved.

The same concept is developed for adding or subtracting two distinct SPP sources. Fig. 2(a) shows the schematic diagram of a four-port adder/subtractor metallic nanostructure for adding or subtracting two different SPP waves. It is assumed that the ports-1, and -3 are being excited by two equal amplitude sources with phase difference of $\Delta\varphi=\varphi_2-\varphi_1=\pi/2$ radians, and considering the ports-2 and -4 as the output ports.

Here, φ_1 and φ_2 represent the phase of SPP_1 and SPP_2 sources. As mentioned in the basic two port structure, the distance of all terminal ports to the outer edge of the ring resonator is considered to be equal to 250 nm. The geometrical parameters are identical to the mentioned basic structure shown in Fig. 1(a). The method of even and odd equivalent circuits can be used for analyzing the operation of the four-port module. Considering the transmission matrix of each element of

the structure as *[M]=[ABCD]*, the transmission matrix for l_1 and l_3 waveguides can be found [20]:

$$[M]_j = \begin{bmatrix} \cos\theta_j & iZ_0 \sin\theta_j \\ iY_0 \sin\theta_j & \cos\theta_j \end{bmatrix} \quad (2)$$

where j = 1, 3, and Y_0 is the characteristic admittance of the MIM waveguide. According to Fig. 2 (b) for the open circuited l_2 the transmission matrix is:

$$[M]_2 = \begin{bmatrix} 1 & 0 \\ iY_0 \tan\theta_2 & 1 \end{bmatrix} \quad (3)$$

Thus, the total transmission matrix of the even equivalent circuit can be written as:

$$[M]_{even} = [M]_1 \times [M]_2 \times [M]_3 \times [M]_2 \times [M]_1 \quad (4)$$

The input SPP from port-1 (SPP_1) passing through $l_3=\lambda_r/4$, takes $\theta_3=-\pi/2$ radians phase shift, while SPP_3 (the input SPP at port-3) experiences a $\pi/2$ radians phase difference in comparison with the SPP_1, due to passing through an additional $\lambda_r/4$ transmission line.

Similarly, according to Fig. 2(c), the transmission matrix for the odd equivalent circuit is:

$$[M]_{odd} = [M]_1 \times [M']_2 \times [M]_3 \times [M']_2 \times [M]_1 \quad (5)$$

$$[M']_2 = \begin{bmatrix} 1 & 0 \\ -iY_0 \cot\theta_2 & 1 \end{bmatrix} \quad (6)$$

Thus, the input SPPs of ports-1, and -3 are added at port-2 and subtracted at port-4.

3 Results and Discussion

The transmission spectrum of the two-port structure at the output port is depicted in Fig. (3), according to the numerical calculations (solid line). Moreover analytic TLM theory (dashed line), verifies the numerical simulation results. It should be noted that the transmission spectrum of a simple ring filter [11] (circles) is shown in the figure without the ports.

The numerical analysis is performed by two-dimensional FDTD [27], with uniform mesh size of $\Delta x=\Delta y$=5 nm, and a Gaussian SPP source. Furthermore, the dielectric function of silver (Ag) which is dispersive in optical wavelengths is computed using the Drude-Lorentz (DL) classical model with five poles, for accounting the interband transition of the electrons [28].

Regarding Fig. 3 in free space wavelength λ=650, 914 and 1860 nm, which correspond to λ_{SPP}= 530, 820 and 1516 nm, the branched SPP waves are added and subtracted at the output junction port, respectively. This is due to the fact that $\Delta\theta\approx-3\pi$ radian at λ_{SPP}=530 nm, $\Delta\theta$=0 radian at λ_{SPP}= 820 nm, and $\Delta\theta\approx-\pi$ radians at λ_{SPP}=1516 nm. In addition, the odd modes proportional to λ_{SPP}= 530, and 1516 nm are eliminated and the even mode corresponding to λ_{SPP}= 820 nm can be transmitted through port-2 (output port). The results of [11] demonstrate that the simple symmetric ring filter can transmit both the even and odd modes, in contrast with the proposed asymmetric structure which eliminates the odd modes. The difference between the results of numerical calculations, and the TLM theory in the transmission spectrum of Fig. 3, is due to disregarding the impedance discontinuities at the T-junctions [25].

Figs. 4(a) and 4(b) depict the normalized transmission spectrum at port-2 (solid-line) and port-4 (dashed-line) based on the numerical calculations and the TLM theory. According to Fig. 4(a), at λ= 630 nm (or λ_{SPP}=518 nm) a maximum peak, and at λ= 1775 nm (or λ_{SPP}=1535 nm) a relative minimum occurs at port-2, correspondingly. The minimum at λ_0= 1775 nm occurs as the consequence of the phase difference ($\Delta\theta=\pi$ radians) between SPP1 and SPP3. This is due to the passing of SPP1 through l_3 which causes θ_1= -3π/2 radians, and SPP3 through l_2 which causes θ_2= 3π radians. Furthermore, the maximum peak in λ= 630 nm is due to the phase difference of $\Delta\theta\approx-\pi/2$ radians between SPP1 and SPP3.

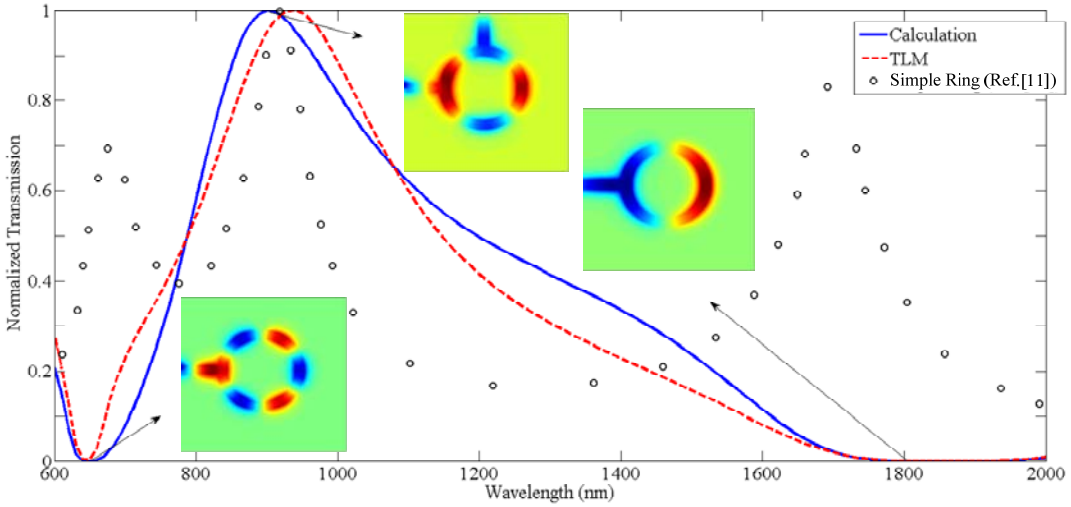

Fig. 3 Normalized transmission spectrum of port-2, obtained from calculations (solid line), TLM theory (dashed line), and the simple ring filter (circles) from Ref. [11]. The two-port MIM module consists of silver with the dielectric layer of air, R_{ave} = 210 nm, and w = 50 nm. The insets show the induced magnetic field at λ = 650, 914, 1860 nm.

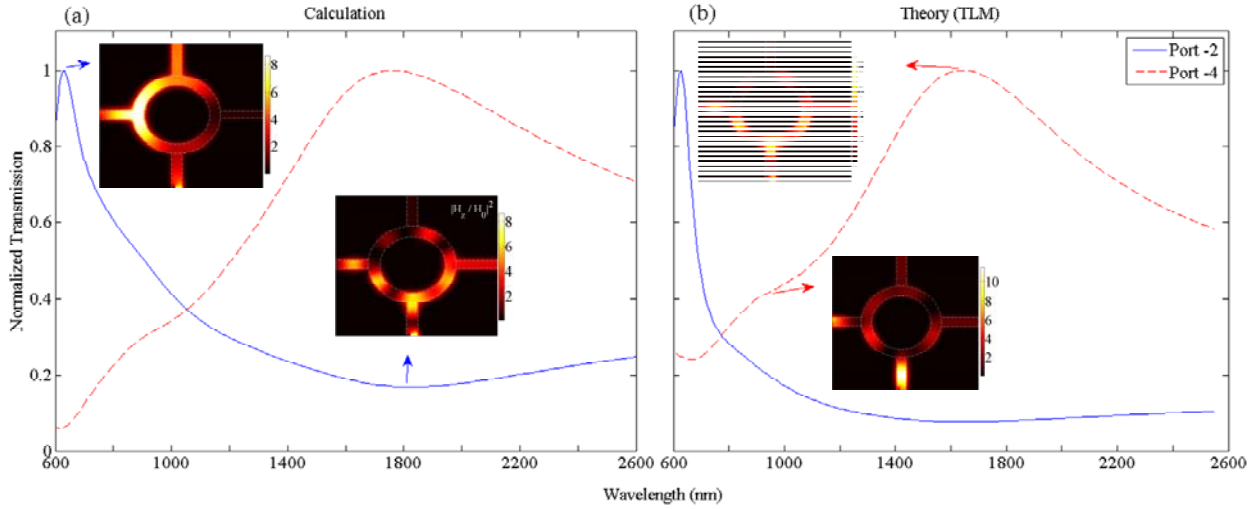

Fig. 4 Normalized transmission spectrum at port-2 (solid-line), and port-4 (dashed-line) obtained from (a) calculations, and (b) TLM theory. The four-port MIM module consists of silver with the dielectric layer of air, R_{ave} = 210 nm, and w = 50 nm. The insets show the induced magnetic field at λ= 630, 1775 nm for port-2, and λ= 901, 1856 nm for port-4.

In addition, the shoulder and the maximum at λ = 901, and 1856 nm are due to $\Delta\theta \approx \pi/2$, and $\Delta\theta$ = 0 radian at λ_{SPP} = 800, and 1660 nm, respectively. Similar to the two-port module, the slight differences between the numerical results and the TLM theory are due to the disregarding the impedance discontinuities at the T-junctions [24].

Figs. 5(a)-(d) show the normalized magnetic field component of H_z at resonant wavelengths of port-2 and port -4. According to Fig. 5(a)-5(d) and considering the number of resonant modes as N, it can be seen that the subtraction and addition operations occur for N=3 at λ=630, 901, and for N=1 it occurs at λ=1775 and 1856 nm, respectively.

Since the addition and subtraction operations at ports-2, and -4 are strongly depend on the phase difference of the input sources, the impact of the phase variations of the input sources on the outputs should be studied. Figures 6(a) and 6(b) illustrate the effect of $\Delta\varphi$= 0 (solid-curve), $\pi/4$ radians (dashed-curve), $\pi/2$ (dash-dotted curve), $3\pi/4$ (circles), and π (squares) radians of the input SPP sources on the behavior of the transmission spectrum at ports-2, and -4, respectively.

According to Fig. 6(a), by increasing $\Delta\varphi$, the first (short-wavelength) and second (long wavelength) resonant peaks are red-shifted at port-2. Moreover, for $\Delta\varphi > \pi/2$ radians the first peak vanishes slightly and converts to a localized minimum. The disappearance of the first peak is due to the elimination of the third order mode by the phase difference. Furthermore, according to Fig. 6(b) by increasing $\Delta\varphi$ the first (short wavelength) and second (long wavelength) resonant peaks are blue shifted. Moreover, similar to the results of Fig. 6(a), for $\Delta\varphi > \pi/4$ radians the second resonant peak vanishes and converts to a minimum peak.

Figs. 7(a) and 7(b) show the effect of $\Delta\varphi$ variations on the first (circles), and second (squares) resonant peaks wavelengths obtained by calculations, and also the first (triangles), and second (deltas) resonant peaks wavelengths obtained from the TLM theory, respectively. According to Figs. 7(a) and 7(b), increasing $\Delta\varphi$ leads to a red shift for the first, and second resonant peaks of the transmission spectrum at port-2, while it results in a blue shift for the resonant peaks at port-4. In fact, these red and blue shifts are due to resonating the ring resonator at other resonant wavelengths in consequence of phase variations of the input SPPs.

Interestingly, for $\Delta\varphi > \pi/2$ radians the second resonant mode disappears slightly at port-4 because of vanishing the resonant modes at these values of $\Delta\varphi$.

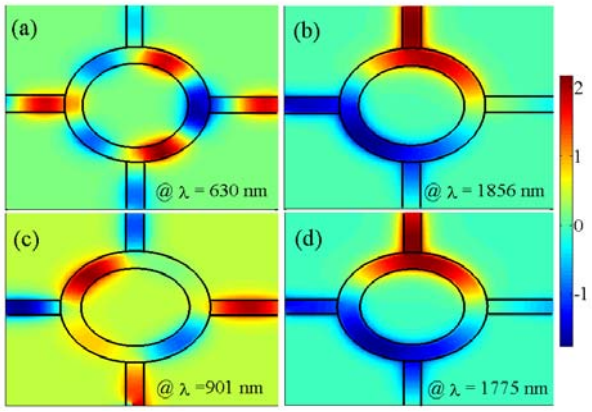

Fig. 5 Real part of the induced magnetic field H_z of the four port module at (a) λ = 630, (b) 1856, (c) 901, and (d) 1775 nm.

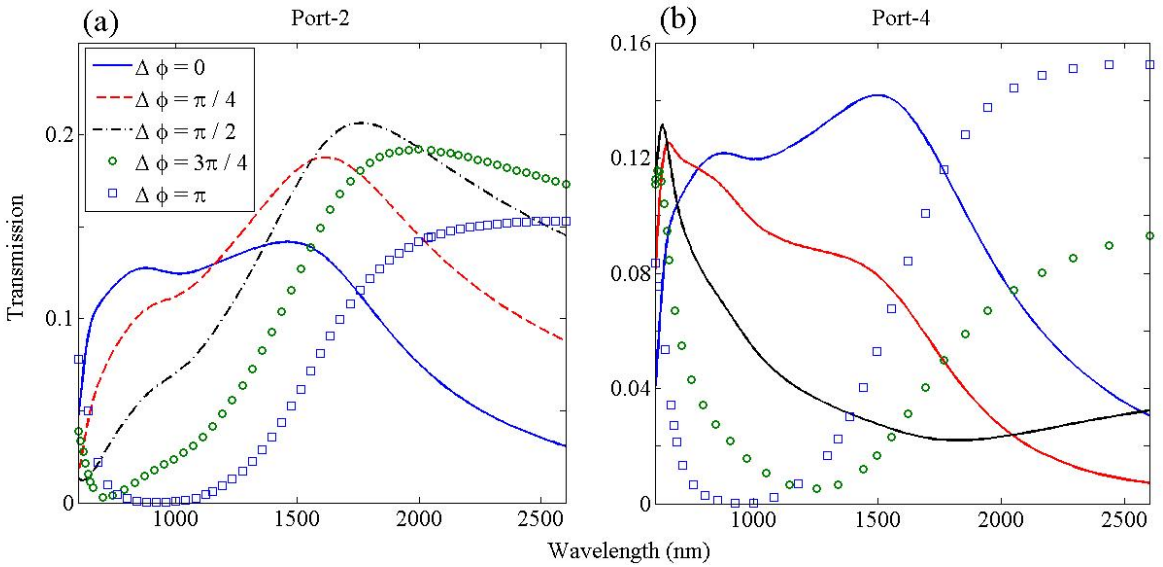

Fig. 6 The normalized transmission spectrum at (a) port-2, (b) port-4 for 0 (solid line), $\pi/4$(dashed line), $\pi/2$ (dash-dotted line), $3\pi/4$ (circles), and π (squares) radians of phase difference between input sources.

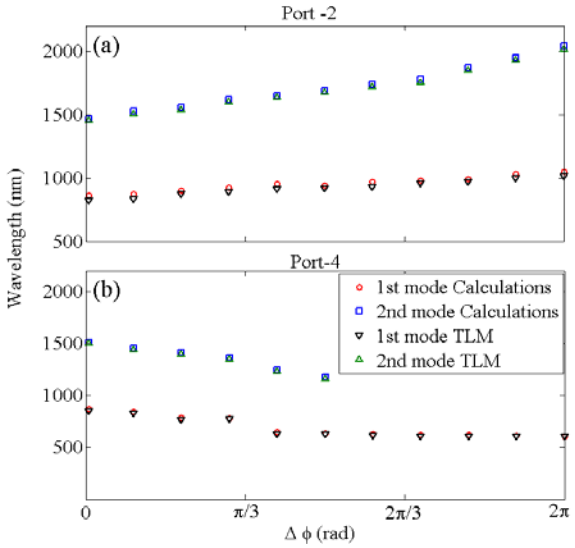

Fig. 7 Variation of the first (circle), and second (square) resonant peaks at (a) port-2, and (b) port-4 using FDTD calculations and the TLM theory (triangles, and deltas) versus the phase difference of the input sources.

4 Conclusion

A plasmonic adder-subtractor module based on a MIM ring resonator is proposed as the building block for arithmetic operations of integrated photonic circuits. The four port adder-subtractor consisted of two input ports and two output ports are designed based on the similar concepts of a two port device. It is shown that the two port device works as a filter which filters the odd modes and transmits the even modes. Moreover, it is demonstrated that by proper excitation of the inputs of the four-port module, the added and subtracted SPP waves of two distinct inputs can be achieved at the output ports. It is found that, the four-port module, the transmission spectrum of the outputs show two individual peaks which can be considered as sum, and difference operations of the input SPPs. Furthermore, it is shown that the functionality of the four-port nanostructure is strongly dependent on the phase variations of the SPP sources. The TLM theory used to verify the operation of the adder/subtractor.

References

[1] E. Ozbay, "Plasmonics: Merging photonics and electronics at nanoscale dimensions," *Science,* vol. 311, pp. 189-193, 2006.

[2] S. A. Maier, P. G. Kik, H. A. Atwater, S. Meltzer, E. Harel, B. E. Koel and A. G. Requicha. "Local detection of electromagnetic energy transport below the diffraction limit in metal nanoparticle plasmon waveguides," *Nat. Materials*, vol. 2, pp. 229-232, 2003.

[3] J. A. Dionne, L. A. Sweatlock, H. A. Atwater, and A. Polman, "Plasmon slot waveguides: Towards chip-scale propagation with subwavelength -scale localization," *Phys. Rev.*, vol. B-73, pp. 0354071-0354079, 2006.

[4] M. Quinten, A. Leitner, J. R. Krenn, and F. R. Aussenegg, "Electromagnetic energy transport via linear chains of silver nanoparticles," *Opt. Lett.*, vol. 23, pp. 1331-1333, 1998.

[5] D. Martin-Cano, M. L. Nesterov, A. I. Fernandez-Dominguez, F. J. Garcia-Vidal, L. Martin-Moreno, and E. Moreno, "Domino plasmons for subwavelength terahertz circuitry," *Opt. Express*, vol. 18, pp. 754-764, 2010.

[6] D. F. P. Pile, and D. K. Gramotnev, "Channel plasmon-polariton in a triangular groove on a metal surface," *Opt. Lett.*, vol. 29, pp. 1069-1071, 2004.

[7] S. I. Bozhevolnyi, V. S. Volkov, E. Devaux, and T. W. Ebbesen, "Channel plasmon-polariton guiding by subwavelength metal grooves," *Phys. Rev. Lett.*, vol. 95, pp. 0468021-0468024, 2005.
[8] D. K. Gramotnev, and D. F. P. Pile, "Single-mode subwavelength waveguide with channel plasmon-polaritons in triangular grooves on a metal surface," *Appl. Phys. Lett*., vol. 85, pp. 6323-6325, 2004.
[9] E. Verhagen, J. A. Dionne, L. Kuipers, H. A. Atwater, and A. Polman, "Near-Field Visualization of Strongly Confined Surface Plasmon Polaritons in Metal-Insulator-Metal Waveguides," *Nano let*, vol. 8, pp. 2925-2929, 2008.
[10] Y. Matsuzaki, T. Okamoto, M. Haraguchi, M. Fukui, and M. Nakagaki, "Characteristics of gap plasmon waveguide with stub structures," *Opt. Express*, vol. 16, pp. 16314-16325, 2008.
[11] T. B. Wang, X. W. Wen, C. P. Yin, and H. Z. Wang, "The transmission characteristics of surface plasmon polaritons in ring resonator," *Opt. Express*, vol. 17, pp. 24096-24101, 2009.
[12] B. Yun, G. Hu, and Y. Cui, "Theoretical analysis of a nanoscale plasmonic filter based on a rectangular metal–insulator–metal waveguide," *J. Phys. D Appl. Phys.*, vol. 43, 385102, 2010.
[13] M. Janipour, M. A. Karami, R. Sofiani, and F. Kashani, "A novel adjustable plasmonic filter realization by split mode ring resonators," *Journal of Electromagnetic Analysis and Applications*, 2013.
[14] G. Wang, H. Lu, X. Liu, D. Mao, and L. Duan, "Tunable multi-channel wavelength demultiplexer based on MIM plasmonic nanodisk resonators at telecommunication regime," *Opt. Express*, vol. 19, pp. 3513-3518, 2011.
[15] R. Zia, J. A. Schuller, A. Chandran, and M. L. Brongersma. "Plasmonics: the next chip-scale technology," *Mat. Today*, vol. 9, pp. 20-27, 2006.
[16] P. Mühlschlegel, H.-J. Eisler, O. J. F. Martin, B. Hecht, and D. W. Pohl, "resonant optical antennas," *Science*, vol. 10, pp. 1607-1609, 2005.
[17] J. A. Dionne, L. A. Sweatlock, H. A. Atwater, and A. Polman, "Planar metal plasmon waveguides: frequency-dependent dispersion, propagation, localization, and loss beyond the free electron model," *Phys. Rev.*, B, vol. 72, pp. 0754051-07540511, 2005.
[18] R. Zia, M. D. Selker, P. B. Catrysse, and M. L. Brongersma, "Geometries and materials for subwavelength surface plasmon modes," *J. Opt. Soc. Am. A*, vol. 21, pp. 2442-2446, 2004.
[19] L. Novotny and B. Hecht, *Principles of Nano-Optics*, Cambridge University, 2006.
[20] Q. Liu, Z. Ouyang, C. J. Wu, "All optical half adder based on cross structures in two-dimensional photonic crystals", *Opt. Express*, vol. 16, pp. 18992-19000, 2008.
[21] H. Wei, Z. Wang, X. Tian, M. Käll, and H. Xu, "Cascaded logic gates in nanophotonic plasmon networks," *Nat. Commun*, vol. 2(387), pp. 1-5, 2011.
[22] Y. Fu, X. Hu, C. Lu, S. Yue, H. Yang, and Q. Gong, "All-optical logic gates based on nanoscale plasmonic slot waveguides," *Nano let*, vol. 12, pp. 5784-5790, 2012.
[23] A. Dolatabady, and N. Granpayeh, "All optical logic gates based on two dimensional plasmonic waveguides with nanodisk resonators", *Journal of optical society of korea*, vol. 16, pp. 432-442, 2012.
[24] I. Zand, A. Mahigir, T. Pakizeh, and M. S. Abrishamian, "Selective mode optical nanofilters based on plasmonic complementary split ring resonators," *Opt. Express*, vol. 20, pp. 7516-7525, 2012.
[25] D. M. Pozar, *Microwave engineering*, 3rd ed., Wiley, 2009.
[26] I. Wolf, and N. Knoppik, "Microstrip ring resonator and dispersion measurement on microstrip lines," *Elec. Lett.*, vol. 7, pp. 779-781, 1971.
[27] A. Taflove, and S. C. Hagness, *Computational Electrodynamics: The Finite-Difference Time-Domain Method*, Artech House, 2005.
[28] M. Janipour, T. Pakizeh, and F. Hodjat-Kashani, "Strong optical interaction of two adjacent rectangular nanoholes in a gold film," *Opt. Express*, vol. 21, pp. 31769-31781, 2013.

Mohsen Janipour was born in Iran. He received the Ph.D. degree from Iran University of Science and Technology, Tehran, Iran in 2014. His research interests include: nanoantenna, optical interaction of nanoparticles and nanoholes, and microwave and radio frequency circuits.

Mohammad Azim Karami was born in Tehran, Iran. He received the Ph.D. degree in Electronic engineering from Technical University of Delft (TU Delft), the Netherlands in 2011. From 2011, he is an assistant Professor in the Electronics group of Iran University of Science and Technology (IUST). His research interests include: plasmonic and optoelectronic devices design and implementation.

Ali Zia was born in Shiraz. He received his M.Sc. Degree in Electrical engineering from Iran University of Science and Technology (IUST), Tehran, Iran in 2013. His research interests include plasmonic circuits.